J. Fluid Mech. (1981), *vol.* 103, *pp.* 1–22
Printed in Great Britain

Nonlinear wave–kinetic interactions in irreversibly reacting media

By G. E. ABOUSEIF AND T. Y. TOONG
Mechanical Engineering Department, Massachusetts Institute of Technology

(Received 29 June 1979 and in revised form 11 April 1980)

Nonlinear wave–kinetic interactions are analysed by examining the propagation of finite-amplitude waves in a gaseous medium undergoing non-equilibrium exothermic reaction. An exact nonlinear wave equation is developed, and the various coupling mechanisms are identified.

An approximate equation, which takes into account the chemical and transport effects, is derived for high-frequency weak nonlinear waves. The equation is numerically integrated to predict the amplification rates of weak shock pulses and changes in their wave forms under different reaction conditions.

Dramatic nonlinear amplification is predicted for mixtures of high activation energies. Furthermore, the amplification rates are enhanced with increased shock strength and pulse duration. In the latter instance, a threshold value is identified, above which wave amplification is a maximum.

1. Introduction

It has been established both theoretically and experimentally that irreversible exothermic reactions are capable of amplifying acoustic pressure disturbances. Several earlier theoretical studies (Toong 1972· Toong *et al.* 1975; Garris, Toong & Patureau 1975; Clarke 1977, 1978*a*, *b*) have examined the chemical effects on the propagation of sound waves in spatially homogeneous irreversibly reacting mixtures. These studies have dealt mainly with linearized theories of acoustic–kinetic interactions; nevertheless, substantial amplification of the acoustic waves was found possible. Furthermore, the linearized quasi-steady theory developed by Toong and his co-workers was successful in predicting the observed sound amplification rates when the ratio Ω of the characteristic chemical time to the wave period is large (Patureau, Toong & Garris 1977). However, if Ω is decreased below a critical value, which depends on the reaction kinetic parameters, theory predicts larger amplification rates (Garris *et al.* 1975). Recent experimental results by the authors (Abouseif, Toong & Converti 1979) corroborated these theoretical predictions.

The experimental results have also indicated that, at high amplification rates, sound waves may develop into weak shocks in rather short time intervals, thereby introducing both hydrodynamic and chemical-kinetic nonlinear effects. Thus, a nonlinear model becomes essential for predicting the temporal evolution of the wave amplitudes and structure during the reaction history. Such information should enable one to assess the role of nonlinear wave–kinetic interactions in various reacting flow instabilities (Toong 1974).

0022-1120/81/4602-2820 $02.00

Clarke (1978*b*) and Blythe (1979) examined the case where the wave amplitude is comparable in magnitude to the inverse (dimensionless) activation energy (β) of the reacting medium. Although such assumption implies significant nonlinear kinetic effects and, consequently, leads to dramatic increases in amplification rates, it does not necessarily require that hydrodynamic nonlinearities be quite as important. Indeed, activation energies may be large enough to satisfy this condition with rather weak finite-amplitude waves. In addition, Clarke focused his attention on the 'awkward' shock-fitting problem in the presence of an irreversible reaction, which is essential when transport effects are neglected.

This paper will first examine the possible nonlinear aspects of wave–kinetic interactions in irreversibly reacting media. An exact nonlinear pressure wave equation will be developed to identify the various possible nonlinear effects. The linearized theory will then be reviewed and compared with the experimental results. In the second part of the paper, an approximate wave equation will be developed for weak nonlinear high-frequency waves. The equation is valid for $\delta \equiv p'/p_0 \leqslant 1{\cdot}0$ and $\delta\beta \lesssim 1$. Moreover, the dissipation mechanisms (transport effects) are accounted for. This, in effect, eliminates the need for the shock-fitting process.

Finally, the approximate wave equation is numerically integrated to predict the amplification rates of weak shock pulses and changes in their wave forms. In particular, the effects of pulse strength and duration, reaction activation energy and thermicity are examined, and the results are compared with the linear predictions.

2. Possible nonlinear effects

The importance of an exact wave equation for non-equilibrium reacting flows is self-evident as regards identifying the additional nonlinear effects (or terms) that do not appear in acoustic perturbation problems. The derivation is most easily made upon noting that, in the absence of shock fronts, the transport effects may be neglected, and the governing equations may thus be transformed [see appendix A] into the following nonlinear wave equation,

$$\frac{D^2p}{Dt^2} - a_f^2\frac{\partial^2 p}{\partial x^2} = -\frac{a_f^2}{\rho}\frac{\partial p}{\partial x}\frac{\partial \rho}{\partial x} + \frac{1}{\rho^2}\frac{D\rho}{Dt}\frac{D}{Dt}(\rho^2 a_f^2) + \frac{D}{Dt}\left[\gamma_f p \frac{D\ln R_f}{Dt}\right] - \frac{D}{Dt}\left[\rho(\gamma_f - 1)\sum_{j=1}^{n} h_j \frac{DY_j}{Dt}\right], \tag{1}$$

where p and ρ are, respectively, pressure and density, a_f is the isentropic frozen sound speed, and γ_f is the frozen specific-heat ratio; Y_j and h_j are the mass fraction, and the enthalpy of formation of the jth specie respectively. R_f is the frozen mean specific gas constant of the n-species gaseous mixture.

The left-hand side of (1) is the classical wave equation, with the exception that local time derivatives are replaced by material derivatives, which account for nonlinear convection. The right-hand side displays all the source or forcing terms, which can affect the wave propagation. The first term represents nonlinear steepening and scattering effects. The second term accounts for the changes in a characteristic flow impedance ρa_f. Such changes may result from variations in the mean or local values of gas temperature, density and concentration. The third term accounts for the changes in the mixture composition, as manifested by the mean gas constant R_f. Finally, the last term represents the effect of reaction thermicity. It is by far the most

important element in wave-kinetic coupling, particularly in exothermic flows, and some remarks on its nature are in order.

As stated in (A 6), the reaction rate w_j is, in general, a function of the mass fraction $Y_j (j = 1, \ldots n)$, density ρ, and temperature T. Thus, perturbations of these flow variables, whether due to pressure or thermal fluctuations, should result in perturbations of the reaction rates. In order to illustrate this further, one may apply the Arrhenius kinetics for the case of a single reacting species, namely

$$w = -\rho \frac{DY}{Dt} = K[\rho Y]^m \exp(-E/\bar{R}T), \tag{2}$$

where m, E and K are the reaction order, activation energy, and specific reaction rate, respectively. Upon perturbing (2), one obtains

$$\frac{w'}{w_0} = \left[1 + \frac{\rho'}{\rho_0} + \frac{Y'}{Y_0} + \frac{\rho' Y'}{\rho_0 Y_0}\right]^m \exp(\beta T'/T) - 1 \tag{3}$$

and

$$w_0 = K[\rho_0 Y_0]^m \exp(-\beta). \tag{4}$$

In exothermic flows, $\beta/m \gg 1$ (typical values are $\simeq 10 \to 50$). Since

$$\frac{\rho'}{\rho_0}, \frac{Y'}{Y_0} \simeq O\left(\frac{T'}{T_0}\right), \tag{5}$$

it follows that the highly nonlinear kinetic temperature dependence (namely $\beta T'/T$) will manifest itself at disturbance levels far below those required for the, usually, weak nonlinear density and mass fraction dependence, which is indicated by the reaction order. Moreover, since hydrodynamic nonlinearities manifest themselves strongly when p'/p_0, ρ'/ρ_0, $T'/T_0 \gtrsim O(1)$, while kinetic nonlinearity becomes significant when $\beta T'/T_0 \gtrsim O(1)$ [cf. equation (3)], one may thus encounter several distinct regimes. First, we introduce the disturbance level parameter δ, where

$$\delta \equiv \frac{p'}{p_0} \tag{6}$$

and

$$\frac{\rho'}{\rho_0}, \frac{T'}{T_0} = O(\delta). \tag{7}$$

If $\delta \ll 1$, and $\beta\delta \ll 1$, one may linearize both hydrodynamic and kinetic terms. Such limit was the subject of the extensive linear theoretical analyses of Toong (1972), Toong *et al.* (1975), Garris *et al.* (1975), Clarke (1977, 1978*a*, *b*), and the experimental studies of Patureau *et al.* (1977) and Abouseif *et al.* (1979), who studied the sound amplification in irreversible photochemical hydrogen–chlorine reaction. (The results of this linearized analysis will be reviewed briefly in the following section.)

However, if $\delta \ll 1$, but $\beta\delta \gtrsim O(1)$, one encounters the case where acoustic disturbances may indeed result in kinetic nonlinearity. Under such conditions, it is permissible to linearize the hydrodynamic terms, but not the kinetic terms (Clarke 1979; Blythe 1979). This limit describes the case where linear hydrodynamics (or acoustics) may not necessarily imply linearized kinetics.

Finally, if $\delta \gtrsim O(1)$ and $\beta\delta \gtrsim O(1)$, both hydrodynamic and kinetic nonlinearities should be accounted for.

Interestingly enough, since the nonlinear hydrodynamic terms are proportional to δ^2, while nonlinear kinetic terms follow an exponential behaviour, more than one regime may be encountered in the course of the chemical reaction. The last two cases will be the subject of the following analysis. However, the linear analysis is discussed first.

3. Linear effects

The linear studies focused on the propagation of plane acoustic waves of specified wavelength in a homogeneous, stagnant, lossless gaseous medium of infinite extent, and capable of chemically reacting. At time $t = 0$, a simple one-step exothermic reaction, following Arrhenius kinetics, is initiated. The molecular mass and specific heats of the medium are assumed unchanged by the reaction. In addition, the pressure level δ is presumed to be arbitrarily small to allow for linearized kinetics ($\beta\delta \ll 1$).

Under such conditions, the following set of linear coupled equations can be derived† (Toong *et al.* 1975; Abouseif 1979):

$$\frac{d}{dt}\left(\frac{\tilde{Y}}{Y_0}\right) = \frac{G_{YY}}{t_c}\frac{\tilde{Y}}{Y_0} + \frac{G_{Ys}}{t_c}\frac{\tilde{s}}{c_p} + \frac{G_{Yp}}{t_c}\frac{\tilde{p}}{p_0}, \tag{8a}$$

$$\frac{d}{dt}\left(\frac{\tilde{s}}{c_p}\right) = \frac{G_{sY}}{t_c}\frac{\tilde{Y}}{Y_0} + \frac{G_{ss}}{t_c}\frac{\tilde{s}}{c_p} + \frac{G_{sp}}{t_c}\frac{\tilde{p}}{p_0}, \tag{8b}$$

$$\frac{d^2}{dt^2}[(\tilde{p}/p_0)/T_r] + \omega^2[(\tilde{p}/p_0)/T_r] = \frac{d^2(\tilde{s}/c_p)}{dt^2}, \tag{8c}$$

where $\tilde{Y}$, $\tilde{s}$, and $\tilde{p}$ are the amplitudes of the mass fraction, entropy, and pressure perturbations, respectively; c_p is the specific heat at constant pressure. The instantaneous characteristic chemical time, t_c, is defined as

$$t_c \equiv T_0/(dT_0/dt); \tag{9}$$

ω is the instantaneous acoustic frequency, given by

$$\omega = \omega_i(T_r)^{\frac{1}{2}}, \tag{10}$$

where

$$T_r \equiv T_0/T_{0,i} \tag{11}$$

and subscripts (0) and (i) designate, respectively, the instantaneous mean, and initial values. The influence coefficients, G_{ik}, in (8) represent the chemical effects and, thus, are dependent on the various kinetic parameters, as shown in table 1. D_{II} is Damköhler's second similarity group, given by

$$\mathrm{D_{II}} \equiv \frac{Y_0 \Delta H}{c_p T_0}, \tag{12}$$

where ΔH is the enthalpy of reaction, and is assumed constant throughout the reaction history.

3.1. *High-frequency limit (quasi-steady conditions)*

Upon examining equations (8a, b), one observes that when the acoustic wave period (defined as the inverse of acoustic frequency) satisfies the relationship

$$t_w = \omega^{-1} \ll (t_c/G_{Yp};\ t_c/G_{sp}) \tag{13}$$

† It should be noted that the equations are written here in terms of dimensional time.

$G_{YY} = (1-m)/\gamma D_{II}$	$G_{sY} = m/\gamma$
$G_{Ys} = [m-1-\beta]/\gamma D_{II}$	$G_{ss} = (\beta-m)/\gamma$
$G_{Yp} = [1-m-\beta(\gamma-1)]/\gamma T_r D_{II}$	$G_{sp} = [m+\beta(\gamma-1)-\gamma]/\gamma T_r$

TABLE 1. Chemical influence coefficients.

or, equally, when the non-dimensional frequency (which represents the ratio of chemical to acoustic time)

$$\Omega \equiv t_c \omega \gg (G_{Yp}, G_{sp}), \tag{14}$$

the rates of change in the mass fraction and entropy fluctuations are governed primarily by the pressure perturbations. Equations (8*a*) and (8*b*) are then reduced to

$$\frac{d}{dt}\left(\frac{\tilde{Y}}{Y_0}\right) \simeq \frac{G_{Yp}}{t_c}\frac{\tilde{p}}{p_0}, \quad \frac{d}{dt}\left(\frac{\tilde{s}}{c_p}\right) \simeq \frac{G_{sp}}{t_c}\frac{\tilde{p}}{p_0}. \tag{15a,b}$$†

Consequently, one may demonstrate that the instantaneous amplitude of the incident wave is given by

$$\frac{\tilde{p}}{\tilde{p}_i} = \exp\left\{\int_{t_i}^{t} A(t)\,dt\right\}, \tag{17a}$$

where A, the amplification rate, is given by the expression (Abouseif 1979)

$$A(t) = \frac{1}{2\gamma T_0}\frac{dT_0}{dt}\left[m+\beta(\gamma-1)+\frac{\gamma}{2}\right]. \tag{17b}$$

Equation (14) depicts the high-frequency limit, which corresponds to high acoustic frequencies and/or slow reaction rates. Under such 'quasi-steady' conditions, wave amplification is merely due to the response of the reaction rate to the 'forcing' acoustic perturbations. It should be noted, however, that the result obtained by Clarke (1978*a*) is slightly different from that of (17*b*) because of the different kinetic model employed in his analysis.

Figure 1 summarizes the results of the extensive experimental studies reported by Patureau *et al.* (1977) and the authors (1979), utilizing the hydrogen–chlorine photochemical reaction [$\beta_i = 8{\cdot}9$, $m \simeq 1{\cdot}0$]. The figure compares the observed amplification rates $\Delta\alpha$ with the predictions of the quasi-steady theory, using two-cycle sound bursts, standing waves, and weak N-shocks. One observes good agreement over a range of $\delta = 10^{-5} \to 10^{-2}$, and $\Omega_i \simeq 5000 \to 300$.

3.2. *Low-frequency limit (non-quasi-steady conditions)*

At lower acoustic frequencies and faster reaction rates, when Ω becomes comparable to the chemical influence coefficients G_{ik}, the quasi-steady results break down. The

† Under such conditions,

$$\frac{\tilde{Y}}{Y_0}, \frac{\tilde{s}}{c_p} = O[(\tilde{p}/p_0)/\Omega], \tag{16}$$

thus making the contributions from the other two forcing terms on the right-hand sides of (8*a*) and (8*b*) negligible. Note also the scattered pressure waves are of $O(\tilde{s}/c_p)$.

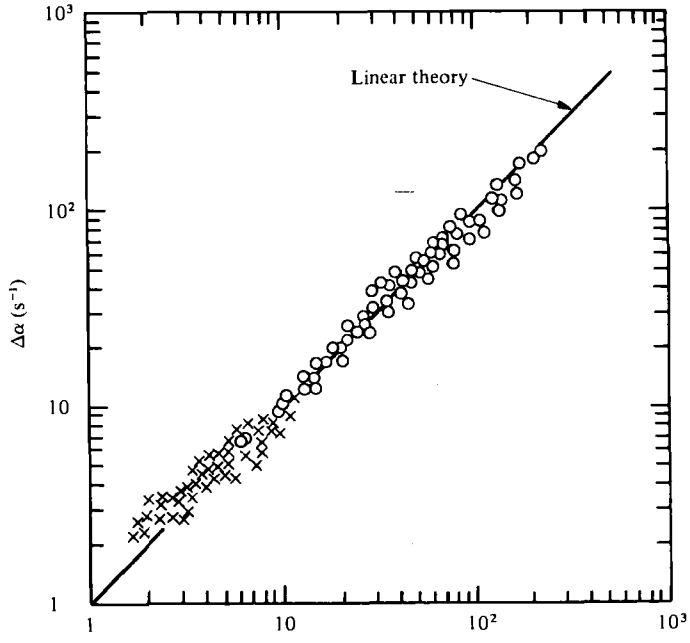

FIGURE 1. Observed sound amplification rate *versus* predicted rate for tone-burst and standing-wave experiments (×), and N-shock experiments (○).

magnitudes of the entropy and mass fraction fluctuations, as well as the scattered waves, become of the order of the incident pressure level. Consequently, the fluctuations in the entropy production and specie consumption may greatly exceed their values in the quasi-steady limit, thereby leading to stronger coupling between acoustics and kinetics.

Recalling (8a) and (8b), one observes that when

$$t_w \propto O\left(\frac{t_c}{G_{Yp}}, \frac{t_c}{G_{sp}}\right) \tag{18a}$$

or, equally, when

$$\Omega \propto O(G_{Yp}, G_{sp}) \tag{18b}$$

the rates of change in the fluctuations of the entropy and mass fraction would also be proportional to, and thus dependent on, their own magnitudes. The most interesting feature about this fact is that it leads to the exponential growth of these variables. This enhances the reaction rate perturbations, and, hence, energy release. Since the latter constitutes the origin of wave amplification, stronger effects should be expected.

This observation may be further illustrated by noting that $\tilde{s}$ is a measure of the irreversible heating effect due to perturbations of the chemical reaction. At low frequencies, this irreversible heating may become sufficiently large, when compared to the reversible acoustic heating, to trigger thermal instability, which is characteristic of irreversible exothermic reactions. This instability will further accelerate the rate of entropy production, thereby augmenting the amplification rates.

Numerical computations (Garris *et al.* 1975; Abouseif 1979) for non-quasi-steady conditions have indeed predicted significant increases in amplification rates. Furthermore, the experimental results by the authors (1979) have corroborated these theoretical findings.

The following analysis will examine the behaviour of high-frequency weak nonlinear waves, in particular, when $\delta \leqslant 1$, $\beta\delta \lesssim 1$, and $\Omega \gg 1$.

4. Nonlinear effects, high-frequency limit

The objective of deriving the exact wave equation (1), notwithstanding the formidable task of solving it, was essentially to reveal all the possible nonlinear hydrodynamic and chemical-kinetic effects. In this section, an approximate equation will be derived for high-frequency weak nonlinear waves. The effects of viscosity and thermal conductivity are accounted for in order to accommodate shock fronts and, thus, eliminate the necessity of the shock-fitting process. However, the coefficients of viscosity and thermal conductivity are assumed constant throughout the reaction history.

4.1. *Physical model and considerations*

The physical model considered comprises a plane finite-amplitude compression wave of specified initial wavelength λ_i, and headed by a shock front (the assumption is made that the wavelength is much greater than the shock-front thickness). The wave is travelling in a homogeneous, stagnant gaseous medium of infinite extent, and capable of chemically reacting. Similarly to the linear model, a simple one-step irreversible reaction is initiated at time $t = 0$. Furthermore, the reaction rate is assumed to be of zeroth order, with an Arrhenius specific reaction rate. A higher-order reaction ($m > 0$) would introduce the concentration dependence, thereby complicating the analysis to a great extent. However, as mentioned earlier, the nonlinear temperature dependence (accounted for in the rate expression) is far more crucial than the concentration dependence, particularly at high activation energies. In addition, the molecular mass and specific heats of the medium are assumed unchanged by the reaction. The effect of changes in mixture composition are, therefore, not considered in the following analysis.

It is most helpful to note that the wave equation, (1), takes account of waves travelling in both directions. Thus, considering an initially right-travelling wave, one should be able, in principle, to reduce this equation to a uni-directional wave equation, with an error proportional to the strength of the generated left-travelling waves. As indicated by (1), scattering may occur in diabatic flows due to pressure–density interactions, whenever density or entropy pockets are formed. However, reaction-stimulated left-travelling waves may also occur due to perturbations in the chemical reaction. This may be seen if one recalls that a reacting particle, essentially, resembles a monopole which has no directional preference. Hence, when a right-travelling wave perturbs a reacting medium, the additional energy release (or entropy production) generates two equal and opposite wavelets. While the right-travelling wavelets lead to amplification of the original wave (whenever the phase requirement is met) the left-travelling wavelets merely modify the flow field behind the shock front.

In fact, entropy production by any physical process would invariably result in pressure waves. A simple illustration may be seen in wave reflection at a shock front,

due to viscous and thermal transport effects (Lighthill 1950). Thus, an estimate of the strength of these stimulated left-travelling waves is certainly essential to provide a confident assessment of the validity of an approximate uni-directional wave equation.

4.2. *Characteristic equations*

In order to accomplish this, the governing equations are rearranged in the following characteristic form:

$$\frac{Dp}{Dt^+}+\rho a\frac{Du}{Dt^+}=(\gamma-1)[q+\phi+w\Delta H]+a\mu_t\frac{\partial^2 u}{\partial x^2} \tag{19a}$$†

valid along positive characteristics C^+, where $dx^+/dt^+ = u+a$;

$$\frac{Dp}{Dt^-}-\rho a\frac{Du}{dt^-}=(\gamma-1)[q+\phi+w\Delta H]-a\mu_t\frac{\partial^2 u}{\partial x^2} \tag{19b}$$†

valid along negative characteristics C^-, where $dx^-/dt^- = u-a$; D/Dt^+ and D/Dt^- are the characteristic operators; ϕ and q are the dissipation function and heat conduction terms, respectively [see (A 10a) and (A 13)]. The viscosity μ_t is given by

$$\mu_t = \tfrac{4}{3}\mu+\mu_b,$$

where μ and μ_b are the coefficients of shear and bulk viscosity, respectively.

The rate of entropy production is given by (Prigogine 1967)

$$\frac{Ds}{Dt}=\frac{1}{\rho T}[q+\phi+w\Delta H] \tag{19c}$$

valid along particle paths p, where $dx/dt = u$.

Equations (A 12) and (19c) may be combined and integrated along p to yield a relationship between ρ, p and s, namely

$$\rho = Bp^{(1/\gamma)}\exp(s/2c_p) \tag{20}$$

where B is a constant. It follows immediately from (A 9) and (A 11f) that the speed of sound a, and gas temperature T are given by

$$a = (\gamma/B)^{\frac{1}{2}}p^{(\gamma-1)/2\gamma}\exp(s/2c_p), \tag{21a}$$

$$T = \frac{p^{(\gamma-1)/\gamma}}{RB}\exp(s/c_p). \tag{21b}$$

Considering the physical model, then any flow quantity Q may be written as

$$Q(x,t) = Q_0(t)+Q'(x,t), \tag{22}$$

where Q_0 is the spatial mean value, and Q' is the perturbation, being the difference between the local and mean values of Q. Combining (19) and (22), one obtains the spatial mean equations, given by

$$u_0 = 0, \quad \rho_0 = \text{constant}, \quad \frac{Dp_0}{Dt^+}=\frac{Dp_0}{Dt^-}=\frac{dp_0}{dt}=(\gamma-1)w_0\Delta H, \tag{23a,b,c}$$

† Subscript f was eliminated in accordance with the physical model, where R and γ were assumed constant.

$$\rho_0 T_0 \frac{ds_{c,0}}{dt} = w_0 \Delta H, \tag{23d}$$

$$w_0 = \begin{cases} K \exp(-\beta), & p_{0,i} \leqslant p_0 < p_{0,f}, \\ 0, & p_0 = p_{0,f}, \end{cases} \tag{23e}\dagger$$

$$\frac{ds_{v,0}}{dt} = 0, \quad q_0 = \phi_0 = 0; \tag{23, f, g}$$

s_c and s_v are the entropy production due to chemical reaction, and transport effects, respectively, and satisfy the following equations

$$s = s_c + s_v, \quad \rho T \frac{Ds_c}{Dt} = w \Delta H, \quad \rho T \frac{Ds_v}{Dt} = q + \phi. \tag{24a, b, c}$$

Similarly, the perturbation equations are given by

$$\frac{Dp'}{Dt^+} + \rho a \frac{Du'}{Dt^+} = (\gamma - 1)[q' + \phi' + w' \Delta H] + a \mu_t \frac{\partial^2 u'}{\partial x^2}, \tag{25a}$$

$$\frac{Dp'}{Dt^-} - \rho a \frac{Du'}{Dt^-} = (\gamma - 1)[q' + \phi' + w' \Delta H] - a \mu_t \frac{\partial^2 u'}{\partial x^2}, \tag{25b}$$

$$\left(\rho T \frac{Ds_c}{Dt}\right)' = w' \Delta H, \quad \rho T \frac{Ds_v'}{Dt} = q' + \phi', \tag{25 c, d}$$

where q' and ϕ' are given by

$$q' = k \frac{\partial^2 T'}{\partial x^2}, \quad \phi' = \mu_t \left(\frac{\partial u'}{\partial x}\right)^2.$$

This formulation has two advantages. First, since we are concerned with the stimulated left-travelling waves, (25*b*) provides an appropriate means of estimating their strength. Secondly, it is best to consider separately the viscous and chemical contributions to entropy production, because then one may be able to identify the various limitations in both reacting and non-reacting flows.

Now at this stage, we may proceed to answer the question concerning the left-travelling waves.

4.3. *Left-travelling waves*

The strength of the left-travelling waves may be estimated by integrating (25*b*) along C^- [see figure 2]. First, the equation is rearranged so as to read

$$\frac{1}{\rho a} \frac{Dp'}{Dt^-} - \frac{Du'}{Dt^-} = \frac{(\gamma - 1)}{\rho a}[q' + \phi'] - \eta_t \frac{\partial^2 u'}{\partial x^2} + \frac{(\gamma - 1)}{\rho a} w' \Delta H, \tag{26}$$

where η_t is given by

$$\eta_t \equiv \mu_t / \rho.$$

† Note from (23*c*) and (23*d*) that, for a zeroth-order reaction, $p_0(t)$ and $T_0(t)$ do not approach their final values asymptotically (as when $m > 0$), but rather at a finite rate. These final values (namely, $p_{0,f}$ and $T_{0,f}$) correspond to $Y_0 = 0$ (complete depletion of the reactant) or reaction completion. Thus, when $Y_0 = 0$ (or equally when $p_0 = p_{0,f}$), w_0 becomes zero and remains zero thereafter.

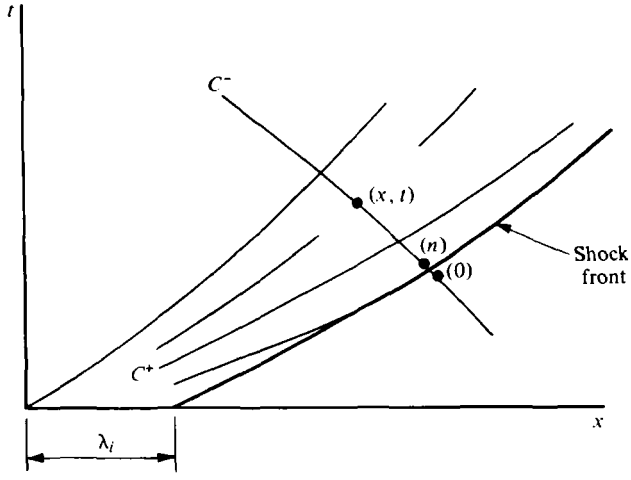

FIGURE 2. The (x, t) plane showing the shock pulse, and the characteristic directions.

Should the flow field be shockless and non-reacting (i.e. homentropic), the right-hand side of (26) vanishes, and one may integrate the left-hand side to yield the classical Riemann invariant; namely

$$\frac{2}{(\gamma-1)}[a-a_0]-u'_h=0 \tag{27a}$$

or

$$\frac{2}{(\gamma-1)}a_0[(1+\delta)^{(\gamma-1)/2\gamma}-1]-u'_h=0, \tag{27b}$$

where use was made of (20) and (21a) with $s=0$. The quantity u'_h is the velocity perturbation due to a pressure perturbation, δ, under homentropic conditions. It should be emphasized that the vanishing right-hand sides of (27a) and (27b) imply that no signal is propagating along C^- or, alternatively, no left-travelling waves are generated.

In the presence of chemical reactions and transport effects, however, the right-hand side of (27b) should comprise terms of $O(s'/c_p)$; as evidenced by both the right-hand side of (26), and the entropy dependence of the impedance ρa appearing in the same equation [see appendix B]. In particular, one obtains in this case [cf. (B 8)]

$$u'(x,t)=\frac{2a_0}{(\gamma-1)}\left[(1+\delta)^{(\gamma-1)/2\gamma}\exp\left(\frac{s'}{2c_p}\right)-1\right]+O\left(a_0\frac{s'}{c_p}\right). \tag{28}$$

After combining (27b) and (28), it transpires that

$$\begin{aligned}u'(x,t)-u'_h(x,t)&=\frac{2a_0}{(\gamma-1)}(1+\delta)^{(\gamma-1)/2\gamma}\left[\exp\left(\frac{s'}{2c_p}\right)-1\right]+O\left(a_0\frac{s'}{c_p}\right)\\&=O\left(a_0\frac{s'}{c_p}\right).\end{aligned} \tag{29}$$

This, in effect, demonstrates that the strength of the left-travelling waves is of the order of the magnitude of the total entropy perturbation s'/c_p just like the linear case under quasi-steady conditions (cf. footnote on p. 5).

In the next section, such entropy production will be considered.

4.4. *Entropy production*

By virtue of the Rankine–Hugoniot relations, entropy production within shock fronts (due to transport phenomena) is solely dependent on the shock strength δ. On the other hand, entropy production due to chemical reactions has to be evaluated strictly according to (25*c*). The latter may be rearranged so as to read

$$\frac{Ds_c'}{Dt} = \frac{1}{\rho T}[w' - \delta w_0]\,\Delta H$$

$$\sim \frac{1}{\rho_0 T_0}[w' - \delta w_0]\,\Delta H. \tag{30}$$

For a zeroth-order Arrhenius expression, equation (3) reduces to

$$\frac{w'}{w_0} = \exp(\beta T'/T) - 1, \tag{31a}$$

where T'/T is given by [cf. (21*b*)]

$$\frac{T'}{T} = 1 - (1+\delta)^{(1-\gamma)/\gamma} \exp\left(-\frac{s'}{c_p}\right). \tag{31b}$$

Combining (23*c*), (30) and (31), one obtains

$$\frac{1}{c_v}\frac{Ds_c'}{Dt} \sim \frac{1}{T_0}\frac{dT_0}{dt}[\exp(\beta T'/T) - 1 - \delta]. \tag{32}$$

Equation (32) may be integrated approximately, along the path of a reacting particle traversing the shock pulse, to provide an upper bound for s_c'; namely

$$\left[\frac{s_c'}{c_v}\right]_{\max} < \frac{t_w}{t_c}[\exp(\beta T'/T) - 1 - \delta]_{\max}, \tag{33}$$

where the bracket represents the maximum value within the wave and t_w and t_c are, respectively, the wave period and the characteristic chemical time. The latter is defined by (9).

In terms of characteristic frequencies f_w and f_c, (33) may be expressed as

$$\left[\frac{s_c'}{c_v}\right]_{\max} < \frac{1}{\Omega}[\exp(\beta T'/T) - 1 - \delta]_{\max}, \tag{34}$$

where Ω is the dimensionless wave frequency, defined as [cf. (14)]

$$\Omega \equiv f_w/f_c = t_c/t_w. \tag{35}$$

4.5. *Weak nonlinear high-frequency waves*

When $\delta \leqslant 1$, it may be shown that (for $\gamma = 1{\cdot}6$), $s_v'/c_p < 10^{-2}$ (Lighthill 1956). On the other hand, for $s_c'/c_p \ll 1$, (34) requires

$$\Omega \gg [\exp(\beta'/T) - 1 - \delta]_{\max}. \tag{36}$$

This, in essence, implies high-frequency waves and/or slow reaction rates. (It should be noted that, when $m = 0$ and $T'/T \ll 1$, (36) reduces to (14).)

Although (36) does not, explicitly, place any upper limit on the exponent $\beta T'/T$, nevertheless the physical model does indeed require that $\beta T'/T < 1$. This may be seen by examining (23d), which provides an estimate of the increase in the spatial mean value of s_c during a characteristic wave period t_w. In particular, one obtains that

$$\frac{\Delta s_{c,0}}{c_v} \simeq \frac{w_0 \Delta H}{\rho_0 T_0 c_v} t_w = \frac{1}{\Omega}, \tag{37}$$

where use was made of (23c) and (A 11f). Thus, by combining (34) and (37), it transpires that

$$\frac{[s_c']_{\max}}{\Delta s_{c,0}} < [\exp(\beta T'/T) - 1 - \delta]_{\max}. \tag{38}$$

If $\beta T'/T > 1$, $[s_c']_{\max}$ may greatly exceed $\Delta s_{c,0}$. Since $s_{c,0}$ is a measure of the mean reactedness of the medium, the assumption of a spatial mean value for all the flow variables should break down under such conditions. Consequently, one may conclude, the validity of the physical model mandates that

$$\beta \frac{T'}{T} \lesssim 1. \tag{39}$$

Furthermore, since $T'/T \sim \delta$ according to (31b) when $s'/c_p \ll 1$, then (39) reduces to

$$\beta\delta \lesssim 1. \tag{40}$$

Thus, for weak nonlinear high-frequency waves, and when $\beta\delta \lesssim 1$, (28) may be further manipulated, giving

$$u' \simeq \frac{2}{(\gamma-1)} (1+\delta)^{(\gamma-1)/2\gamma} a_0. \tag{41}$$

Finally, by substituting (20), (21) and (41) into the perturbation equation along the positive characteristics C^+, (25a), one obtains the approximate nonlinear wave equation

$$\frac{\partial \delta}{\partial t} + a_0 \Gamma(\delta) \frac{\partial \delta}{\partial x} = \frac{\gamma D_{\mathrm{II},i}}{2(p_0/p_{0,i})} \frac{w'}{\rho_0} - B(\delta) \frac{d \ln p_0}{dt} + D(\delta), \tag{42}$$

where $\Gamma(\delta)$, $B(\delta)$ and $D(\delta)$ are given by

$$\Gamma(\delta) \equiv \frac{(\gamma+1)}{(\gamma-1)} [F(\delta) - 1], \tag{43}$$

$$B(\delta) \equiv \frac{\delta}{2} + \frac{\gamma}{2(\gamma-1)} G(\delta) [F(\delta) - 1], \tag{44}$$

$$D(\delta) \equiv \frac{\gamma}{(\gamma-1)} \eta_t \left[F(\delta) \frac{\partial^2 F(\delta)}{\partial x^2} + 2 \left(\frac{\partial F(\delta)}{\partial x} \right)^2 \right] + \frac{\gamma k}{2\rho_0 c_p} \frac{\partial^2 F^2(\delta)}{\partial x^2}, \tag{45}$$

with

$$F(\delta) \equiv (1+\delta)^{(\gamma-1)/2\gamma}, \quad G(\delta) \equiv (1+\delta)^{(\gamma+1)/2\gamma}; \tag{46), (47}$$

$D_{\mathrm{II},i}$ is the initial value of Damköhler's second similarity group [cf. (12)], and given by

$$D_{\mathrm{II},i} \equiv \frac{Y_{0,i} \Delta H}{c_p T_{0,i}} = (T_{0,f} - T_{0,i})/\gamma T_{0,i}, \tag{48}$$

where $T_{0,f}$ is the spatial mean gas temperature at reaction completion. It is important to note that (42) was derived in terms of δ, rather than p', because the former is the relevant nonlinear parameter.

The left-hand side of (42) displays a uni-directional wave operator, which takes into account nonlinear convection through the term $\Gamma(\delta)$. It is precisely this term that results in wave steepening and, thus, formation of shock fronts. The latter, in turn, will enhance the dissipation effects as indicated by $D(\delta)$. The first two terms on the right-hand side of the equation manifest the nature of wave–kinetic interactions. In particular, they demonstrate the effect of reaction-rate perturbations, and mean pressure rise on wave amplification. These two chemical terms vanish at and after reaction completion since w_0 vanishes under these conditions [see (23*c*), (23*e*) and (31*a*)].

In order to assess the balance between these various effects, (42) is numerically integrated, and the results are presented and discussed in the following section.

5. Numerical results and discussion

It is emphasized again that the ultimate objective of this work is to explore the role of wave–kinetic coupling in the inception and sustenance of instabilities in reacting flows. Perhaps foremost amongst these instabilities is the intriguing phenomenon of gaseous detonation. Interestingly enough, all detonable mixtures share the exclusive property of high activation energy. The latter, however, may drop considerably by changing the reaction conditions of a specific mixture, thereby suppressing its detonability. Thus, by focusing one's attention on a specific chemical system with variable kinetics, one may indeed shed light on the conditions leading to wave amplification and, thereon, triggering the instability.

The hydrogen–chlorine reaction offers such advantageous feature. When photo-initiated, the activation energy is approximately 5·26 kcal/mol (Abouseif *et al.* 1979). However, at elevated temperatures ($\sim$ 1000 °C), thermal initiation raises the activation energy to approximately 54 kcal/mol (Abouseif 1979). In the latter instance, detonation has been consistently observed (Lee *et al.* 1972).

The following analysis will examine the effect of both activation energy and reaction thermicity (mixture dilution) on nonlinear wave amplification. In addition, the effects of initial wave strength and pulse duration will be analysed.

5.1. *Low activation energy*

The approximate wave equation, (42), was numerically integrated (see appendix C), using an explicit finite-difference scheme, to provide the amplification rate of weak shock pulses, of various initial strengths and durations, travelling in a reacting mixture with $\beta_i = 8{\cdot}9$, and thermicity $D_{\mathrm{II},i} = 1{\cdot}9$. Both values, which are based on an initial temperature of $T_{0,i} = 300$ °K, represent typical photo-initiated hydrogen–chlorine mixtures. However, one should note that the above thermicity is approximately 20 % of the stoichiometric value.

The computations were performed for three initial shock strengths (namely, $\delta_i = 0{\cdot}1$, 0·3 and 0·6) and the temporal peak amplitude changes are shown in figure 3 (see figure 4 for the temporal evolution of the wave profile for $\delta_i = 0{\cdot}3$). The figure indicates that, when $\delta_i \leqslant 0{\cdot}1$, the amplification rates are identical to those predicted by the linear theory [cf. (17)]. Increasing the shock strength further would only slightly

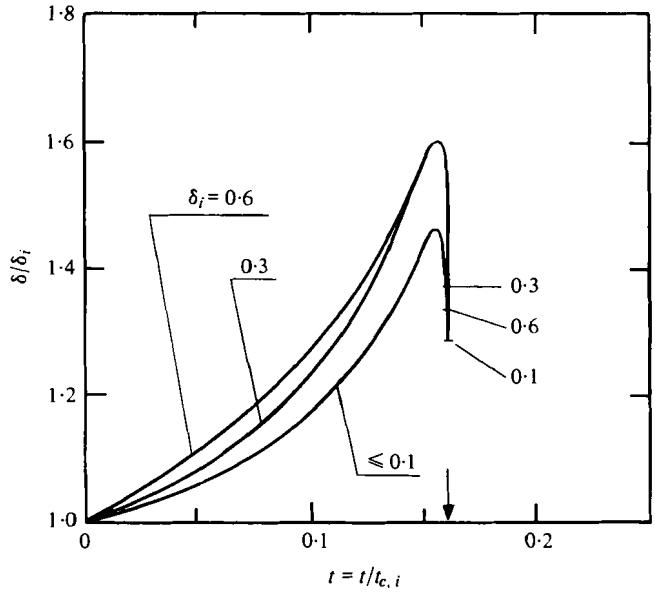

FIGURE 3. Temporal peak amplitude changes for shock pulses of various initial strengths. Parameters employed: $\beta_i = 8{\cdot}9$, $D_{\mathrm{II},i} = 1{\cdot}9$, $(t_{w,i}/t_{c,i}) = 0{\cdot}039$. ↓ indicates reaction completion.

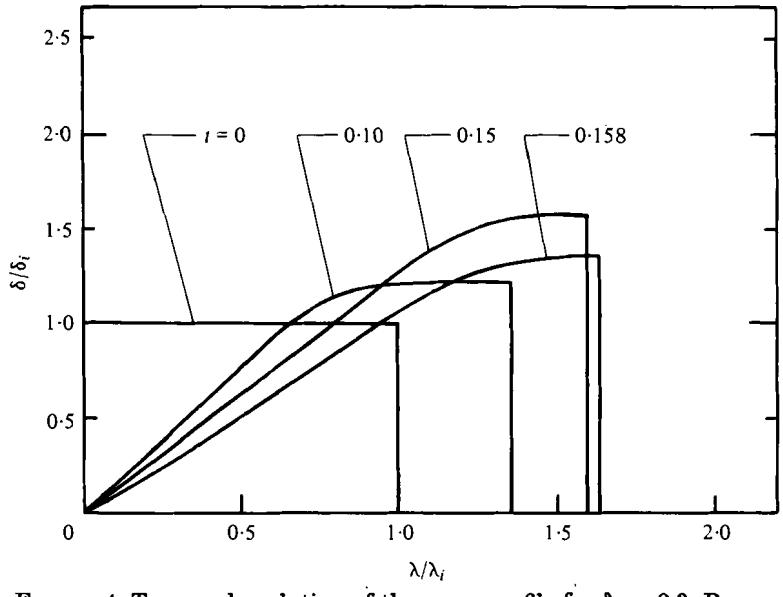

FIGURE 4. Temporal evolution of the wave profile for $\delta_i = 0{\cdot}3$. Parameters employed: $\beta_i = 8{\cdot}9$, $D_{\mathrm{II},i} = 1{\cdot}9$, $(t_{w,i}/t_{c,i}) = 0{\cdot}039$.

enhance the amplification rates. Moreover, when $\delta_i = 0{\cdot}6$, one observes that the final shock strength, at reaction completion, is less than that of the case where $\delta_i = 0{\cdot}3$.

The most striking fact abot this result is, merely, its occurrence despite the large increase in the magnitude of the nonlinear kinetic terms ($\beta_i\delta_i \simeq 5{\cdot}3$ when $\delta_i = 0{\cdot}6$, as compared to $\beta_i\delta_i \simeq 0{\cdot}9$ when $\delta_i = 0{\cdot}1$). Nonetheless, the explanation is found most

easily if one recalls the following factors. First, when $\delta \geqslant 0{\cdot}1$, nonlinear convection becomes increasingly significant. Consequently, the shock pulse ultimately develops into an N-wave (cf. figure 4). Prior to the N-wave formation, the shock front is not influenced by the trailing expansion wave. However, once the N-wave is fully developed, the amplification rate may suffer a considerable drop due to the attenuation effect of the expansion wave. The rapidity of this event depends primarily on the initial shock strength and the pulse width.

Secondly, one may rewrite (5) so as to read

$$\beta = \beta_i T_{0,i}/T_0, \tag{49}$$

which illustrates the fact that β drops significantly as the reaction proceeds towards completion (where $\beta \simeq 2{\cdot}2$), thereby reducing, considerably, the contribution of the nonlinear kinetic terms.

Lastly, it is important to recall that w', which constitutes the origin of wave amplification, is proportional to w_0 as demonstrated by (31a). The latter, in turn, is dependent on the kinetic parameters β and K [cf. (23e)].

Thus, the final outcome, as far as net amplification is concerned, depends on these three factors simultaneously. For the kinetic parameters chosen, it appears that, when $\delta_i = 0{\cdot}6$, the attenuation effect of the expansion wave offsets the additional contribution due to the nonlinear kinetic terms. The latter, themselves, also experience significant reduction as the mean temperature increases. It should be emphasized, however, that, with different kinetic parameters, the outcome may differ greatly.

To illustrate further the effect of nonlinear convection on wave amplification, the temporal peak amplitude changes are shown in figure 5 for shock pulses of various initial durations $t_{w,i}$, but identical initial strength, namely $\delta_i = 0{\cdot}3$. The figure indicates that, below a threshold initial duration of $t_{w,i}/t_{c,i} = 0{\cdot}039$, the shock strength falls significantly short of its maximum attainable value, if there were no attentuation.

Finally, one observes a common feature displayed by figures 3–5, namely the rapid drop of shock strength near reaction completion. This results whenever the time rate of increase of the mean pressure p_0 exceeds that of p', and occurs, in this case, at a temperature ratio of $T_r = 2{\cdot}76$, or a corresponding thermicity of $D_{\mathrm{II},i} = 1{\cdot}1$. Employing a higher thermicity ($D_{\mathrm{II},i} = 1{\cdot}9$ or $T_r = 4{\cdot}0$) did, in fact, attenuate, rather than amplify, the shock pulse, as depicted by figures 3–5. Thus, although finite exothermicity is a necessary condition for wave amplification, one should note that employing stoichiometric mixtures may not necessarily enhance wave amplification.

5.2. *High-activation energy*

With thermal initiation, however, the hydrogen–chlorine reaction acquires a dimensionless activation energy $\beta_i \simeq 20$ [based on an initial temperature $T_{0,i} = 1300\,^{\circ}\mathrm{K}$]. However, a thermicity identical to the previous case ($D_{\mathrm{II},i} = 1{\cdot}9$) was employed to facilitate the comparison.

Figure 6 shows the effect of initial shock strength on wave amplification at the shock front. The figure indicates that, whereas $\delta_i \leqslant 0{\cdot}01$ corresponds to the linear limit, higher shock strengths result in dramatic increases in the amplification rates. This is attributed, in large part, to the highly nonlinear temperature dependence of the reaction rate, which accelerates considerably even under the slightest perturbation.

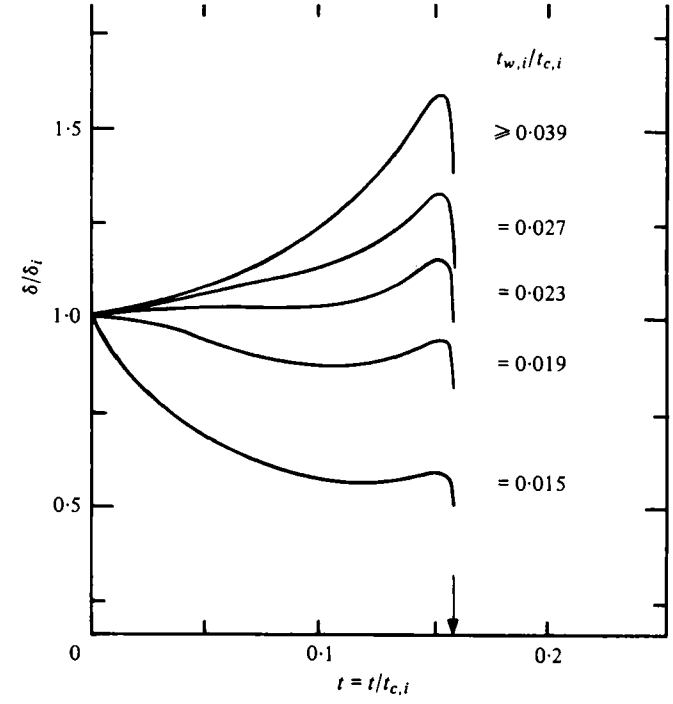

FIGURE 5. Temporal peak amplitude changes for shock pulses of various initial duration $t_{w,i}$. Parameters employed: $\beta_i = 8{\cdot}9$, $D_{\mathrm{II},i} = 1{\cdot}9$, $\delta_i = 0{\cdot}3$. ↓ indicates reaction completion.

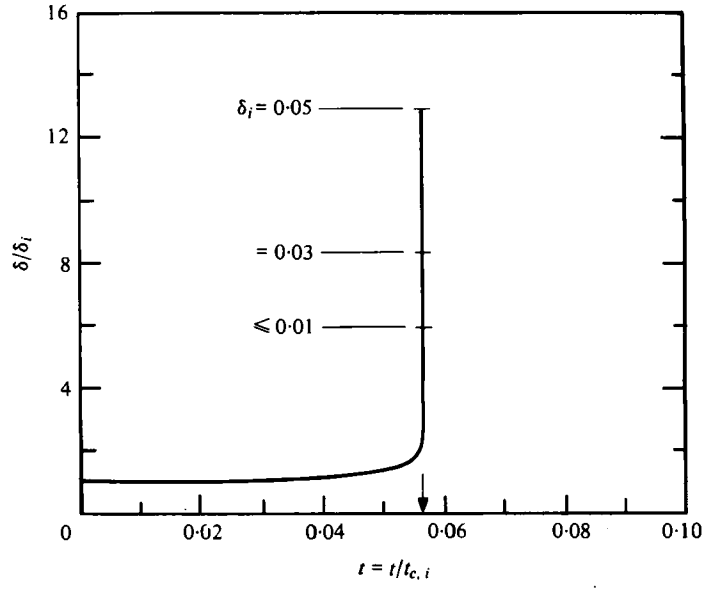

FIGURE 6. Temporal peak amplitude changes for shock pulses of various initial strength. Parameters employed: $\beta_i = 20$, $D_{\mathrm{II},i} = 1{\cdot}9$, $(t_{w,i}/t_{c,i}) = 0{\cdot}015$. ↓ indicates reaction completion.

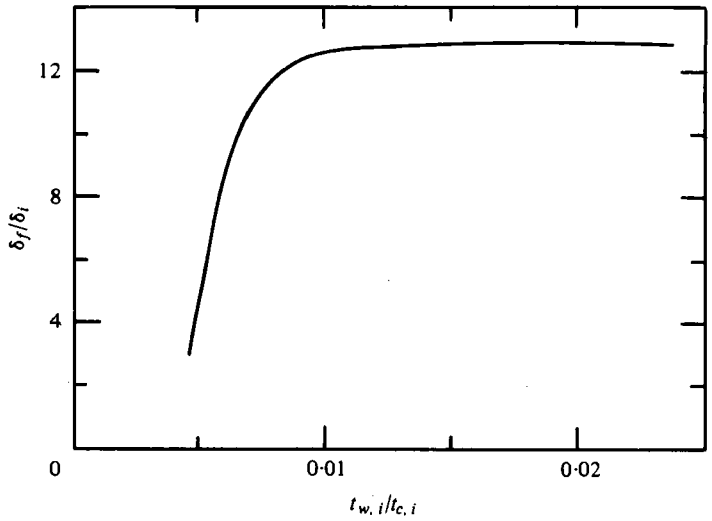

FIGURE 7. Effect of initial pulse duration, $t_{w,i}$, on shock strength at reaction completion, δ_f. Parameters employed: $\beta_i = 20$, $D_{\mathrm{II},i} = 1{\cdot}9$, $\delta_i = 0{\cdot}05$.

Moreover, at these relatively weak shock strengths, the role of nonlinear convection is largely reduced. Although initial shock strengths exceeding $\delta_i = 0{\cdot}05$ were not examined (because $\beta_i\delta_i$ would then exceed unity, thereby invalidating the physical model), nevertheless, it is believed that increasing the shock strength further would invariably enhance the amplification rates (Abouseif 1979).

In contrast to figure 3, figure 6 demonstrates that δ increases monotonically, and quite rapidly, near reaction completion.† Should one employ a stoichiometric thermicity ($D_{\mathrm{II},i} = 2{\cdot}4$), one would obtain a slight increase in the final shock strength.

The effect of pulse duration, for a given initial strength ($\delta_i = 0{\cdot}05$), is shown in figure 7. Again, one identifies a threshold duration ($t_{w,i}/t_{c,i} \sim 0{\cdot}01$) below which the amplification rates suffer considerable reduction.

The present results, and those of Clarke (1979), do suggest very strongly that nonlinear wave–kinetic interactions, in irreversible exothermic reactions with high activation energy, lead to dramatic amplification of pressure disturbances. The finding of a threshold pulse duration for maximum amplification may also shed some light on the necessary requirements for the onset of instabilities in reacting flows.

7. Conclusions

The present study has examined the nonlinear coupling between exothermic chemical reactions and gas dynamics. When $\delta < 1{\cdot}0$, $\beta\delta \lesssim 1{\cdot}0$ and $\Omega \gg 1$, an approximate unidirectional nonlinear model may be used in lieu of the exact wave equation. The model, which incorporates the dissipation mechanisms, eliminates the need for the shock-fitting process. Numerical integration of the equation for different reaction conditions has revealed the following features:

(*a*) Nonlinear wave–kinetic coupling results in significant increases in wave

† Note that the criterion for reaction completion is the depletion of reactant (namely, $Y_0 = 0$).

amplification. In particular, reacting mixtures of high activation energies may lead to dramatic increases in amplification rates, even at low shock strengths.

(*b*) Although exothermicity is a necessary condition for wave amplification, employing stoichiometric mixtures does not necessarily enhance the amplification rates and, consequently, the maximum attainable shock strength at reaction completion.

(*c*) A threshold pulse duration exists, whose specific value varies with initial amplitude level and kinetic parameters. Below this minimum value, the amplification rates would be reduced significantly.

The results presented in this paper may be of relevance to instability problems such as those related to direct initiation of detonation and transition from deflagration to detonation. The interaction between weak shock waves and the reaction zone, or flame, which leads to dramatic shock amplification, may indeed trigger and sustain these instabilities.

Appendix A. Governing equations

Conservation equations

The governing equations in a one-dimensional, visous, thermally conducting, chemically reacting gaseous mixture of n species can be written as follows† (Lighthill 1956; Wood & Kirkwood 1957):

$$\frac{D\rho}{Dt}+\rho\frac{\partial u}{\partial x}=0, \quad \rho\frac{DY_j}{Dt}+w_j=0, \tag{A 1), (A 2}$$

$$\rho\frac{Du}{Dt}=-\frac{\partial p}{\partial x}+(\tfrac{4}{3}\mu+\mu_b)\frac{\partial^2 u}{\partial x^2}, \tag{A 3}$$

$$\frac{D\rho}{Dt}=\frac{1}{a_f^2}\frac{Dp}{Dt}+\frac{\rho^2\sigma_f}{c_{pf}}\sum_{j=1}^{n}\left[h_j-\frac{c_{pf}}{\sigma_f}\left(\frac{\partial(1/\rho)}{\partial Y_j}\right)_{p,T,Y_l}\right]\frac{DY_j}{Dt}-\frac{\rho^2\sigma_f}{c_{pf}}\left[k\frac{\partial^2 T}{\partial x^2}+\phi\right], \tag{A 4}$$

$$p=\rho\bar{R}T\sum_{j=1}^{n}\frac{Y_j}{M_j}, \quad w_j=w_j(\rho,T,Y_{j=1,n}), \tag{A 5), (A 6}$$

where p, ρ, u and T are, respectively, pressure, density, gas velocity, and gas temperature. The quantities Y_j, w_j, M_j and h_j are the mass fraction, volumetric reaction rate, molecular mass, and enthalpy of formation of the jth specie, respectively. $\bar{R}$ is the universal gas constant. The frozen specific heat c_{pf}, frozen expansion coefficient σ_f, and isentropic frozen sound speed a_f are given by

$$c_{pf}\equiv\left(\frac{\partial h}{\partial T}\right)_{p,Y_j}, \quad \sigma_f\equiv\left(\frac{\partial(1/\rho)}{\partial T}\right)_{p,Y_j}, \quad a_f^2\equiv\left(\frac{\partial p}{\partial\rho}\right)_{s,Y_j}. \tag{A 7), (A 8), (A 9}$$

Here h and s are, respectively, the enthalpy and entropy of the gaseous mixture; μ, μ_b, and k are the shear viscosity, bulk viscosity, and thermal conductivity of the mixture. The dissipation function, ϕ, is given by

$$\phi=\mu_t\left(\frac{\partial u}{\partial x}\right)^2, \tag{A 10a}$$

where

$$\mu_t=\tfrac{4}{3}\mu+\mu_b. \tag{A 10b}$$

† The effects of mass diffusion are not included for simplicity.

For a mixture of perfect gases, it may be shown that

$$c_{pf} = \sum_{j=1}^{n} Y_j (c_p)_j, \quad \sigma_f = (\rho T)^{-1}, \tag{A 11a, b}$$

$$\gamma_f = c_{pf}/(c_{pf} - R_f), \quad R_f = \sum_{j=1}^{n} R_j Y_j = \bar{R} \sum_{j=1}^{n} \frac{Y_j}{M_j}, \tag{A 11c, d}$$

$$a_f^2 = \gamma_f R_f T = \gamma_f p/\rho, \quad p = \rho R_f T \tag{A 11e, f}$$

$$\left(\frac{\partial(1/\rho)}{\partial Y_j}\right)_{p, T, Y_l} = \frac{R_j}{p}, \tag{A 11g}$$

where, again, subscript f denotes frozen conditions. Now, combining (A 4) and (A 11), and rearranging, one obtains

$$\frac{D\rho}{Dt} = \frac{1}{a_f^2}\left\{\frac{Dp}{Dt} + \rho(\gamma_f - 1) \sum_{j=1}^{n} h_j \frac{DY_j}{Dt} - \gamma_f p \frac{D(\ln R_f)}{Dt} - (\gamma_f - 1)[q + \phi]\right\}, \tag{A 12}$$

where

$$q \equiv k \frac{\partial^2 T}{\partial x^2}. \tag{A 13}$$

It should be noted, however, that, while R_f is dependent on Y_j, γ_f is dependent on both Y_j and T.

The nonlinear wave equation

The set of governing equations [(A 1) to (A 3) and (A 12)] are transformed from the (x, t) plane to a (ψ, t) plane, where ψ is the stream function defined by the identities

$$\rho = \left(\frac{\partial \psi}{\partial x}\right)_t, \quad \rho u = -\left(\frac{\partial \psi}{\partial t}\right)_x, \tag{A 14a, b}$$

and ψ satisfies the continuity equation.

Upon changing of co-ordinates, where

$$\left(\frac{\partial}{\partial t}\right)_x = \left(\frac{\partial}{\partial t}\right)_\psi - \rho u \left(\frac{\partial}{\partial \psi}\right)_t, \quad \left(\frac{\partial}{\partial x}\right)_t = \rho \left(\frac{\partial}{\partial \psi}\right)_t, \tag{A 15a, b}$$

the governing equations (without transport effects) become

$$\frac{\hat{\partial}(1/\rho)}{\partial t} - \frac{\hat{\partial} u}{\partial \psi} = 0, \quad \frac{\hat{\partial} u}{\partial t} + \frac{\hat{\partial} p}{\partial \psi} = 0, \tag{A 16), (A 17}$$

$$\frac{\hat{\partial}\rho}{\partial t} = \frac{1}{a_f^2}\frac{\hat{\partial} p}{\partial t} + \frac{1}{a_f^2}\left[\rho(\gamma_f - 1) \sum_{j=1}^{n} h_j \frac{\hat{\partial} Y_j}{\partial t} - \gamma_f p \frac{\hat{\partial}}{\partial t} \ln R_f\right], \tag{A 18}$$

where

$$\frac{\hat{\partial}}{\partial t} \equiv \left(\frac{\partial}{\partial t}\right)_\psi, \quad \frac{\hat{\partial}}{\partial \psi} \equiv \left(\frac{\partial}{\partial \psi}\right)_t. \tag{A 19a, b}$$

From equations (A 16) and (A 17), by cross-differentiation, one eliminates u to obtain

$$\frac{\hat{\partial}^2(1/\rho)}{\partial t^2} + \frac{\hat{\partial}^2 p}{\partial \psi^2} = 0. \tag{A 20}$$

Combining (A 18) and (A 20), it transpires that

$$\frac{\hat{\partial}^2 p}{\partial t^2}-\rho^2 a_f^2\frac{\hat{\partial}^2 p}{\partial \psi^2}=\frac{1}{\rho^2}\frac{\hat{\partial}(a_f^2\rho^2)}{\partial t}\frac{\hat{\partial}\rho}{\partial t}-\frac{\hat{\partial}}{\partial t}\left[\rho(\gamma_f-1)\sum_{j=1}^{n}h_j\frac{\hat{\partial}Y_j}{\partial t}-\gamma_f p\frac{\hat{\partial}}{\partial t}\ln R_f\right]. \quad \text{(A 21)}$$

Finally, by returning to the (x,t) plane, one obtains the nonlinear wave equation,

$$\frac{D^2 p}{Dt^2}-a_f^2\frac{\partial^2 p}{\partial x^2}=-\frac{a_f^2}{\rho}\frac{\partial\rho}{\partial x}\frac{\partial p}{\partial x}+\frac{1}{\rho^2}\frac{D\rho}{Dt}\frac{D(\rho^2 a_f^2)}{Dt}+\frac{D}{Dt}\left[\gamma_f p\frac{D\ln R_f}{Dt}\right]$$
$$-\frac{D}{Dt}\left[\rho(\gamma_f-1)\sum_{j=1}^{n}h_j\frac{DY_j}{Dt}\right]. \quad \text{(A 22)}$$

Appendix B. Left-travelling waves

Integration of (26) along the C^- characteristic provides a relationship between $u'(x,t)$ and $p'(x,t)$. When such relationship is compared to that given by (27*b*), one may estimate the strength of the left-travelling waves due to dissipation and chemical effects. To accomplish this, it is important to notice that the contribution of the dissipation effects is significant only within the shock front, where the effect due to chemical reaction is negligible. The latter is justified on physical grounds, since a chemical reaction requires much more than the few collisions that constitute the shock front.

Hence, the integration of (26) may be split into two parts, namely

$$\int_{(0)}^{(n)}\frac{1}{\rho a}\frac{Dp'}{Dt^-}dt^- -\int_{(0)}^{(n)}\frac{Du'}{Dt^-}dt^- =\int_{(0)}^{(n)}\left\{\frac{(\gamma-1)}{\rho a}[q'+\phi']-\eta_t\frac{\partial^2 u'}{\partial x^2}\right\}dt^- \quad \text{(B 1)}$$

and

$$\int_{(n)}^{(x,t)}\frac{1}{\rho a}\frac{Dp'}{Dt^-}dt^- -\int_{(n)}^{(x,t)}\frac{Du'}{Dt^-}dt^- =\int_{(n)}^{(x,t)}\frac{(\gamma-1)}{\rho a}w'\Delta H\,dt^-, \quad \text{(B 2)}$$

where (n) designates the state just behind the shock front [see figure 2]. Although the integral given by (B 1) is formidable to evaluate, nevertheless, one may obtain an exact relationship between p' and u' across the front merely by considering the Rankine–Hugoniot relations. In particular, one obtains (Lighthill 1956)

$$\frac{u'(n)}{a_0}=\frac{\delta_n}{\gamma\{1+[(\gamma+1)/2\gamma]\,\delta_n\}^{\frac{1}{2}}}. \quad \text{(B 3)}$$

On the other hand, (B 2), combined with (23*c*), may be rearranged to read

$$u'(x,t)-u'(n)=\int_{(n)}^{(x,t)}\frac{p_0}{\rho a}d\delta-(\gamma-1)\int_{(n)}^{(x,t)}\frac{1}{\rho a}[w'-\delta w_0]\,\Delta H\,dt^-. \quad \text{(B 4)}$$

The first integral on the right-hand side of (B 4) may be evaluated with the aid of (20) and (21*a*). Thus, one obtains

$$\int_{(n)}^{(x,t)}\frac{p_0}{\rho a}d\delta=\frac{2}{(\gamma-1)}a_0\left[(1+\delta)^{(\gamma-1)/2\gamma}\exp\left(\frac{s'}{2c_p}\right)-(1+\delta_n)^{(\gamma-1)/2\gamma}\exp\left(\frac{s'_v}{2c_p}\right)\right]$$
$$+O\left(a_0\frac{s'_c}{c_p}\right). \quad \text{(B 5)}$$

The second integral, when combined with (30), may be shown to be of $O(a_0 s_c'/c_p)$. Hence, (B 4) becomes

$$u'(x,t)-u'(n)=\frac{2}{(\gamma-1)}a_0\left[(1+\delta)^{(\gamma-1)/2\gamma}\exp\left(\frac{s'}{2c_p}\right)\right.$$
$$\left.-(1+\delta_n)^{(\gamma-1)/2\gamma}\exp\left(\frac{s_v'}{2c_p}\right)\right]+O\left(a_0\frac{s_c'}{c_p}\right). \quad \text{(B 6)}$$

Finally, combining (B 3) and (B 6), and rearranging, one obtains

$$u'(x,t)=\frac{2}{(\gamma-1)}a_0\left[(1+\delta)^{(\gamma-1)/2\gamma}\exp\left(\frac{s'}{2c_p}\right)-1\right]$$
$$+a_0\left\{\frac{\delta_n}{\gamma\{1+[(\gamma+1)/2\gamma]\,\delta_n\}^{\frac{1}{2}}}-\frac{2}{(\gamma-1)}\left[(1+\delta_n)^{(\gamma-1)/2\gamma}\exp\left(\frac{s_v'}{2c_p}\right)-1\right]\right\}+O\left(a_0\frac{s_c'}{c_p}\right). \quad \text{(B 7)}$$

The second term on the right-hand side of (B 7) is of $O(a_0 s_v'/c_p)$ (Lighthill 1956). Accordingly, (B 7) may be further reduced to

$$u'(x,t)=\frac{2}{(\gamma-1)}a_0\left[(1+\delta)^{(\gamma-1)/2\gamma}\exp\left(\frac{s'}{2c_p}\right)-1\right]+O\left(a_0\frac{s'}{c_p}\right), \quad \text{(B 8)}$$

where $$s'=s_c'+s_v'.$$

Appendix C. Numerical integration

In the finite-difference numerical computations, if the viscous term $D(\delta)$ [cf. (42)] is to be retained, one has to cope with large local gradients. If one is to numerically simulate a shock pulse of amplitude, say, $\delta = 1{\cdot}0$, and of duration $t_w = 10^{-3}$ s (which corresponds to a pulse length of $\lambda_w \sim 30$ cm) travelling in air, one is faced with the problem of dealing with a shock front of thickness $\lambda_s \sim 10^{-5}$ cm, and duration $t_s \sim 3\times 10^{-10}$ s. In order to achieve numerical stability (particularly behind the shock front), one has to use a mesh spacing Δx no greater than $\lambda_s/3$ (Roache 1976), thus requiring approximately 10^7 mesh points in the entire disturbance flow field. The use of such a large number of mesh points is prohibitively expensive.

This difficulty may be overcome by 'artificially' increasing the coefficients of viscosity and thermal conductivity to such values which will result in a 'thicker' shock front of, say, $\lambda_s \sim 0{\cdot}3$ cm, or $t_s \sim 10^{-5}$ s. Correspondingly, the number of mesh points would be approximately 300, thus drastically reducing the computational time. However, in order to justify this procedure, one has to consider, rather carefully, the ratios of the various characteristic times (or length scales) involved.

The problem at hand, for example, suggests three characteristic times. First, the viscous time t_s required for the passage of a fluid particle through the shock front. Second, the flow time t_w required for a fluid particle to traverse the entire pulse length, λ_w. In addition to these, the characteristic chemical timei t_c [see (9)] is involved. In the present theory, two assumptions were explicitly stated. First, it was assumed that $\lambda_w \gg \lambda_s$, or $t_w \gg t_s$ (see § 4.1). The other assumption restricted the theory to high-

frequency waves, for which the ratio of chemical time to pulse duration is much greater than unity (cf. § 4.5). In other words,

$$\frac{t_s}{t_w} \ll 1, \quad \Omega = \frac{t_c}{t_w} \gg 1. \tag{C 1), (C 2}$$

Combining (C 1) and (C 2), one obtains

$$\frac{t_s}{t_c} = \frac{1}{\Omega}\frac{t_s}{t_w} \ll \frac{t_s}{t_w} \ll 1. \tag{C 3}$$

Now one may artificially expand the shock front provided that (C 3) is not invalidated. Thus, for a pulse duration of $t_w = 10^{-3}$ s (which is typical of the values used in the paper), increasing t_s from 3×10^{-10} to 10^{-5} s would not invalidate (C 3), since the new value of t_s/t_w is still much less than 1, but greatly reduces the numerical computations. (In this connection, it is important to note that under different circumstances, particularly when $t_c/t_w < 1$, the maximum allowable artificial shock front duration becomes limited by the condition $t_s/t_c \ll 1$.)

In the present calculations, the shock pulse occupied typically 300–400 mesh points, while the shock front stretched across 4 mesh spacings only. This is the reason why the shock front appears as a discontinuity in figure 4. Furthermore, reducing the mesh spacing by a factor of two did not affect the predictions behind the shock, although the shock width was reduced by the same factor.

This work was supported by the Air Force Office of Scientific Research (AFSC) under grant AFOSR-78-3662.

REFERENCES

Abouseif, G. E., Toong, T. Y. & Converti, J. 1979 *17th Symp. (Int.) on Combustion*, p. 1341. The Combustion Institute.

Abouseif, G. E. 1979 Ph.D. thesis, Massachusetts Institute of Technology.

Blythe, P. A. 1979 *17th Symp. (Int.) on Combustion*, p. 909. The Combustion Institute.

Clarke, J. F. 1977 *J. Fluid Mech.* **81**, 257.

Clarke, J. F. 1978*a* *Acta Astronautica* **5**, 543.

Clarke, J. F. 1978*b* *J. Fluid Mech.* **89**, 343.

Clarke, J. F. 1979 *J. Fluid Mech.* **94**, 195.

Garris, C. A., Toong, T. Y. & Patureau, J. P. 1975 *Acta Astronautica* **2**, 981.

Lee, J. H. *et al.* 1972 *Comb. & Flame* **18**, 321.

Lighthill, M. J. 1950 *Phil. Mag.* **41**, 1101.

Lighthill, M. J. 1956 *Surveys in Mechanics* (ed. G. K. Batchelor and S. H. Davies), p. 250. Cambridge University Press.

Patureau, J. P., Toong, T. Y. & Garris, C. A. 1977 *16th Symp. (Int.) on Combustion*, p. 929.

Prigogine, I. 1967 *Introduction to Thermodynamics of Irreversible Processes*. Wiley-Interscience.

Roache, P. J. 1976 *Computational Fluid Mechanics*. Hermosa.

Toong, T. Y. 1972 *Comb. & Flame*, **18**, 207.

Toong, T. Y. 1974 *Acta Astronautica* **1**, 317.

Toong, T. Y., Arbeau, P., Garris, C. A. & Patureau, J. P. 1975 *15th Symp. (Int.) on Combustion*, p. 87.

Wood, W. W. & Kirkwood, J. G. 1957 *J. Appl. Phys.* **23**, 395.